ELSEVIER

Synthesis and chiroptical properties of (naphthyl)ethylidene ketals of carbohydrates in solution and solid state

Gábor Kerti [a], Tibor Kurtán [a,*], Anikó Borbás [b], Zoltán B. Szabó [b], András Lipták [b], László Szilágyi [a], Zita Illyés-Tünde [a], Attila Bényei [c], Sándor Antus [a,b,*], Masayuki Watanabe [d], Ettore Castiglioni [d], Gennaro Pescitelli [e], Piero Salvadori [e]

[a] *Department of Organic Chemistry, University of Debrecen, PO Box 20, H-4010 Debrecen, Hungary*
[b] *Research Group for Carbohydrates of the Hungarian Academy of Sciences, University of Debrecen, PO Box 55, H-4010 Debrecen, Hungary*
[c] *Institute of Physical Chemistry, University of Debrecen, PO Box 7, H-4010 Debrecen, Hungary*
[d] *JASCO Corporation, Hachioji-shi, Tokyo 192-85387, Japan*
[e] *Università di Pisa, Dipartimento di Chimica e Chimica Industriale, via Risorgimento 35, 56126 Pisa, Italy*

Dedicated to Professor Csaba Szántay on the occasion of his 80th birthday

Abstract

1,3-Dioxolane- and dioxane-type (1- and 2-naphthyl)ethylidene ketals of p-methoxyphenyl α-L-rhamnopyranoside and β-D-glucopyranoside were prepared and their stereochemistry studied by solution and solid-state circular dichroism, X-ray diffraction, and coupled-oscillator CD calculations on the solid-state and MMFF-calculated geometries. Intermolecular exciton-coupled interactions between the nearby aromatic chromophores in the solid state and different conformers in solution and solid state could be identified as the main reason for the difference between solution and solid-state CDs.
© 2007 Elsevier Ltd. All rights reserved.

Keywords: Solid-state CD; Intra- and intermolecular exciton-coupled interactions; 1- and 2-Naphthyl chromophores

1. Introduction

The protecting group strategy is an essential component in the design and synthesis of oligosaccharides.[1,2] One of us has already shown[3] that ketals prepared from acetophenone dimethylacetal and different β-D-gluco-, β-L-arabino- and α-L-rhamnopyranoside derivatives are very useful building blocks for the synthesis of oligosaccharides, since their reductive ring-cleavage by LiAlH$_4$—AlCl$_3$ took place in a stereoselective manner. Recently, it has also been recognized[4,5] that dioxane-type (2-naphthyl)methylene acetals of glycosides show the same property; reaction of their 4,6-O-acetals with AlH$_3$ (LiAlH$_4$—AlCl$_3$) yielded 4-ONAP ethers whereas reagents such as NaCNBH$_3$ or BH$_3$—Me$_3$N—AlCl$_3$ gave 6-ONAP derivatives with excellent regioselectivity. It has also been shown for (2-naphthyl)methylene acetals of glycosides that both the stereochemistry and the direction of the hydrogenolytic cleavage could be safely detected by CD based on the ^1B_b transition of the 2-naphthyl chromophore when another aromatic protective group like benzyl or p-methoxyphenyl was present in the molecule.[6] As a continuation of our work on the chiroptical properties of aromatic chromophores and aromatic ketal protective groups,[6–9] we report herein the synthesis and stereochemical study of 1,3-dioxane- and dioxolane-type (1- or 2-naphthyl)ethylidene ketals of glycosides by using X-ray analysis, solution and solid-state CD measurements, and coupled-oscillator CD calculations.

---

* Corresponding authors. Fax: +36 52 453836.
E-mail address: kurtant@tigris.klte.hu (T. Kurtán).

2. Results and discussion

For the preparation of 1,3-dioxolane-type naphthylethylidene ketals, *p*-methoxyphenyl α-L-rhamnopyranoside (**1**) was selected as starting material. Its reaction with 2-(1,1-dimethoxyethyl)naphthalene (**6**) resulted in the formation of two isomeric (2-naphthyl)ethylidene ketals (1′R)-**2** and (1′S)-**2** in the presence of (+)-10-camphorsulfonic acid, while the reaction with 1-(1,1-dimethoxyethyl)naphthalene (**7**) in the presence of *p*-toluenesulfonic acid (PTS) provided only a single product (1′R)-**4** with high yield (89%). The ketals were characterized as the acetates [(1′R)-**3**, (1′S)-**3**, and (1′R)-**5**], which also allowed the separation of (1′R)-**3** from (1′S)-**3** (Scheme 1).

On the basis of our earlier results,[6] CD spectroscopy seemed a convenient tool for the configurational assignment of the newly formed stereogenic center of the dioxolane ring. For this purpose, the chiroptical properties of analogous dioxolane-type (2-naphthyl)methylene glycoside acetals **8** and **9** were studied first (Fig. 1), the absolute configurations of which had been unambiguously determined earlier.[10] In the absence of a second aromatic chromophore, both (1′S)-**8** and (1′R)-**8** methyl glycosides gave positive CE above 220 nm with significantly different intensities [(1′R)-**8**: 224 nm (19.4), (1′S)-**8**: 223 nm (2.4)]. In the presence of a glycosidic *p*-methoxyphenyl (PMP) group, the ^1B_b band around 225 nm was split to a bisignate CD band in (1′R)-**9** [229 nm (−8.9), 221 nm (13.8)], while (1′S)-**9** gave a positive exciton[11,12] couplet due to interaction of the naphthalene ^1B_b transition with the aryl ^1L_a and ^1B transitions [226 nm (38.2), 216 nm (−1.9), 194 nm (−15.2)] as shown in Figure 1a and Table 1.

The solution CD spectrum of (1′S)-**3**, the (2-naphthyl)ethylidene analogue of (1′S)-**9**, showed a similar positive exciton couplet as (1′S)-**9** (Fig. 1b) suggesting the same stereochemistry. (1′R)-**3** gave a near mirror image spectrum below 240 nm, which confirmed that the absolute configuration of the ketal carbon, reflecting into the exciton coupling between naphthalene ^1B_b and $^1L_a/^1B$ transitions of the p-methoxyphenyl group, determines the CD curve below 240 nm in (1′S)- and (1′R)-**3**.

In contrast, the naphthalene ^1L_a bands of both (1′S)- and (1′R)-**3** were negative regardless of the different absolute configuration of their ketal carbon.

(1′R)-**5**, obtained as a single product in the reaction with 1-(1,1-dimethoxyethyl)naphthalene (**7**), showed a comparatively weak positive CD couplet [225 nm (3.2), 220 nm (−11.6)] around 225 nm, opposite in sign to that of (1′R)-**3**. This corroborates previous results showing that the electric transition moment of the ^1B_b transition of the 1-naphthyl chromophore is perpendicular to that of the 2-naphthyl chromophore in analogous derivatives, which results in opposite CD couplets due to exciton coupling.[13] In addition, the naphthalene ^1L_a band of (1′R)-**5** also had negative CE, as was observed for both (1′S)- and (1′R)-**3**.

In order to confirm unambiguously the configurational assignments of the ketal carbon and reveal the preferred conformation of the naphthyl groups in the solid state, single crystals of (1′R)-**3** and (1′R)-**5** were studied by X-ray diffraction. The X-ray structures of (1′R)-**3** and (1′R)-**5** (Fig. 2) confirmed the (1′R) configuration of the acetal carbon and showed that both 1-naphthyl and 2-naphthyl rings adopt near *perpendicular* conformation with respect to the methyl group, namely, the torsional angles $\omega_{C-2',C-1',C-2'',C-1''}$ and $\omega_{C-2',C-1',C-1'',C-2''}$ were 74.1° and 104.7°, respectively. The negative and positive projection angles θ between the long axes of the naphthyl and phenyl rings in (1′R)-**3** and (1′R)-**5** ($\theta_3 = -77.0°$, $\theta_5 = +55.3°$, looking through the centers) were in accordance with the measured negative and positive CD couplets, respectively, as prescribed by the exciton-coupled CD (ECCD) theory.[11]

According to the hypothesis that CD spectra of bis-chromophoric compounds **3** and (1′R)-**5** are dominated, at least in a certain wavelength range, by the exciton coupling between the two strong chromophores, it should be possible to reproduce them by means of coupled-oscillator calculations. We employed DeVoe's method,[14] a classical all-order treatment widely used for configurational and conformational investigations of organic molecules.[15] Parameters for DeVoe calculations were extracted from chromophore spectra in acetonitrile (naphthalene and 1,4-dimethoxybenzene, DMB),
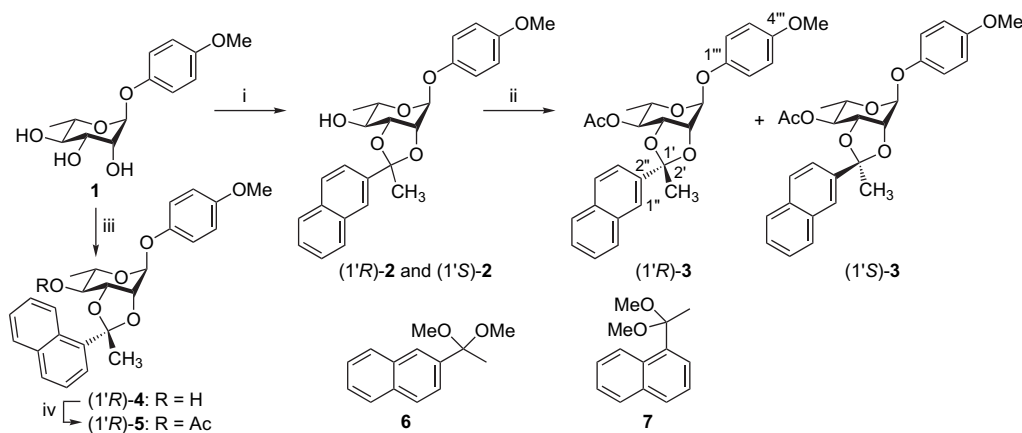
Scheme 1. (i) 2-(1,1-Dimethoxyethyl)naphthalene (**6**)/(+)-10-camphorsulfonic acid/dry MeCN. (ii) Ac₂O/dry pyr., crystallization. (iii) 1-(1,1-dimethoxyethyl)-naphthalene (**7**)/PTS, dry MeCN. (iv) Ac₂O/dry pyr.
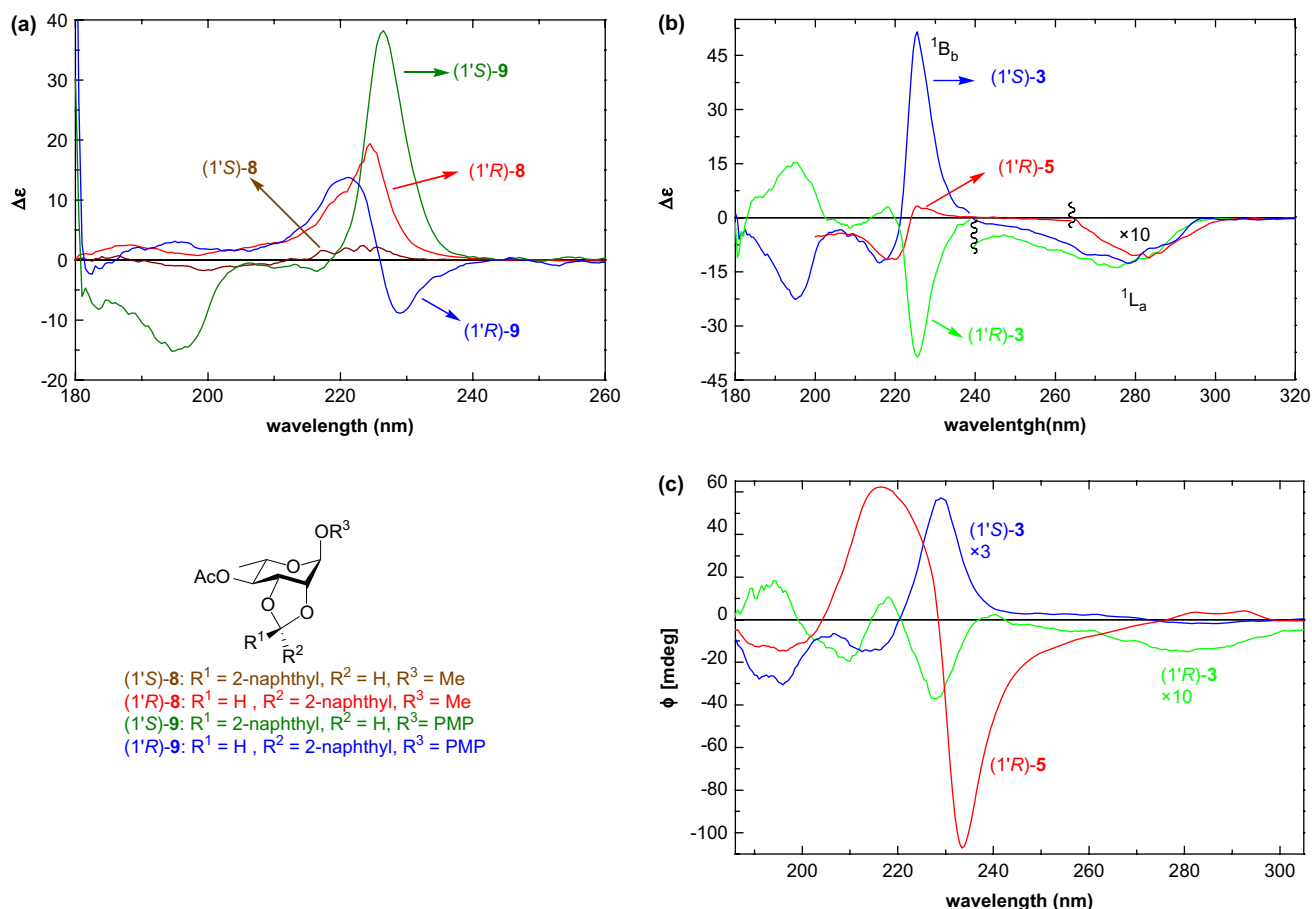
Figure 1. (a) Solution CD spectra of (1′R)- and (1′S)-**8**, (1′R)- and (1′S)-**9**. (b) CD spectra of (1′R)- and (1′S)-**3** and (1′R)-**5** in acetonitrile. (c) Solid-state CD of (1′R)- and (1′S)-**3** and (1′R)-**5** measured as KCl pellet.

supported by ZINDO calculations (see Section 4.3). DeVoe-calculated CD spectra using the solid-state geometries of (1′R)-**3** and (1′R)-**5** are reported in Figure 3. The high-energy region is determined by the coupling between strong dipole-allowed transitions (naphthyl ^1B_b with phenyl ^1L_a and ^1B), and the calculated CD for (1′R)-**3** is in good agreement with the experimental spectrum; the result for (1′R)-**5** is less satisfactory, although the positive couplet is reproduced. On the contrary, the sign for naphthyl ^1L_a CD band is wrongly predicted, indicating that it depends on other mechanisms of optical activity than the coupled-dipole, which cannot be taken into account by the present calculations. One of the advantages of DeVoe-type calculations is that the information of dominant exciton couplings is very easily extracted.[15] For (1′R)-**3**, the CD in the 190–230 nm region is dominated by the couplings between naphthyl ^1B_b transition with all high-energy phenyl transitions ^1L_a (dominant), ^1B_a, and ^1B_b. For (1′R)-**5**, the dominant coupling terms are those between naphthyl ^1B_b and phenyl $^1B_{a,b}$ transitions.

The good agreement between DeVoe calculation results using the X-ray geometry of (1′R)-**3** and the measured solution CD suggested that the solid-state structure was also prevalent in solution and brought the largest contribution to the CD. In order to confirm this hypothesis further and to extend it to (1′R)-**5**, a conformational search with MMFF was run on

(1′R)-**3** and (1′R)-**5**, resulting in four relevant (in terms of exciton coupling) minima for each compound. They differed in the torsional angles $\omega_{C-2',C-1',C-2'',C-1''}$ and $\omega_{C-2',C-1',C-1'',C-2''}$ (either ≈+90° or −90°) for the naphthyl−ketal linkage, and $\omega_{H-1,C-1,O-1,C-1'''}$ (either ≈+40° or −40°) for the DMB−C1 linkage; in all cases, the DMB moiety was planar ($\omega_{C-1,O-1,C-1''',C-2'''} \approx 0°$). Although the overall conformational ensembles for (1′R)-**3** and (1′R)-**5** are of course quite complex, we thought that the four minima would well represent average situations of conformational sets each characterized by a peculiar exciton coupling. Thus, the CDs for the four geometries and their weighted average (relative to MMFF energies) were calculated with DeVoe's method (Fig. 4). For (1′R)-**3**, among the four low-energy conformers considered, the lowest energy one (conf. 1, 50% population at 298 K) resembled the X-ray structure. Both the calculated CD of the lowest energy conformer and the weighted average reproduced well the measured CD below 240 nm, but the opposite sign was calculated for the measured negative CE around 280 nm. For (1′R)-**5**, among the four conformers, the second lowest energy one (conf. 2, population 30%) was similar to the X-ray structure and since it had much more intense CD than the lowest energy conformer, it dominated the CD. However, the contribution from other conformers reduces the overall intensity, bringing it closer to the experimental CD.

Table 1
Solution and solid-state CD data of the studied compounds

Compound	λ [nm] ($\Delta\varepsilon$) for solution and λ [nm] (ϕ)[a] for solid-state CD measurements
(1'R)-3	MeCN: 285sh (−0.9), 282sh (−1.1), 275 (−1.4), 271sh (−1.3), 266sh (−1.1), 225 (−38.7), 218 (3.1), 208 (−2.9), 195 (14.1). KCl: 285sh (−1.4), 280 (−1.5), 228 (−3.7), 218 (1.0), 210 (−2.0), 194 (1.8).
(1'S)-3	MeCN: 283 (−1.1), 279sh (−1.0), 271sh (−0.62), 232sh (10.8), 225 (51.5), 216 (−12.5), 195 (−22.7). KCl: 286 (−0.7), 281sh (−0.6), 229 (19.1), 212 (−5.0), 196 (−10.2).
(1'R)-5	MeCN: 288sh (−0.7), 285sh (−0.8), 278 (−1.3), 268sh (−1.0), 225 (3.2), 220 (−11.6). KCl: 292 (4.0), 282sh (3.5), 260sh (−8.0), 233 (−107.2), 226sh (27.6), 216 (62.3), 195 (−14.75).
(1'R)-8	Hexane: 284 (−0.4), 273 (−0.6), 224 (19.4), 218sh (9.4), 214sh (4.7), 188 (2.5).
(1'S)-8	Hexane: 225sh (2.2), 223 (2.4), 221sh (2.0), 217sh (1.6), 209sh (−0.8), 199 (−1.7).
(1'R)-9	MeCN: 229 (−8.9), 221 (−13.8), 195 (2.9), 182 (−2.3).
(1'S)-9	MeCN: 226 (38.2), 216 (−1.9), 210 (−1.2), 194 (−15.2).
(1'R)-11	MeCN: 283 (−4.4), 274sh (−3.1), 233sh (5.8), 225 (33.3), 218 (−15.3), 216 (−15.0), 211sh (−7.8), 194 (−11.3). KCl: 289sh (1.2),[b] 277 (2.5),[b] 268sh (2.1),[b] 228 (14.6), 225sh (9.5), 215 (−5.4), 191 (−2.9).
(1'S)-12a	MeCN: 293 (1.3), 283sh (0.9), 272sh (0.1), 223 (−39.6), 213sh (−9.1), 209sh (−5.0), 201sh (−3.8), 196sh (12.5), 193 (14.7). KCl: 296 (1.2), 284sh (0.3), 278sh (−0.4), 263sh (−0.9), 227 (−13.1), 201 (−2.3), 192 (3.8).

[a] Values of ellipticity [ϕ (mdeg)] are not corrected for the concentrations.
[b] Measured at higher concentration than the high-energy transition.

The comparison of the measured solid-state CD with the one computed for the solid-state X-ray geometry has recently allowed the determination of the absolute configuration or the conformation of several natural[16−21] and synthetic[22] compounds. We intended to apply this methodology to (naphthyl)-ethylidene ketals as well whose X-ray structures have been determined. Thus the solid-state CDs of (1'R)-3, (1'S)-3, and
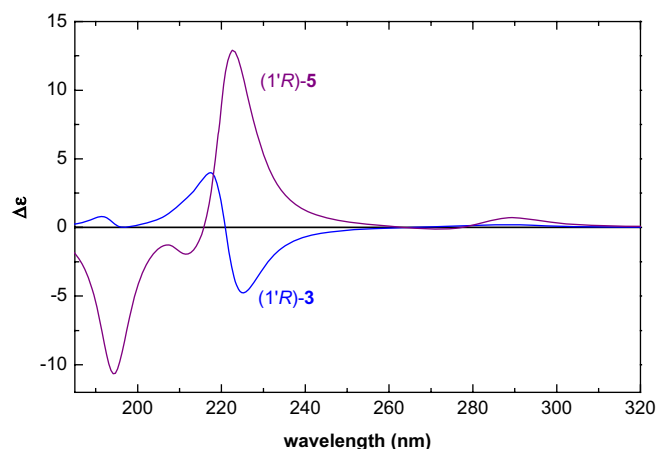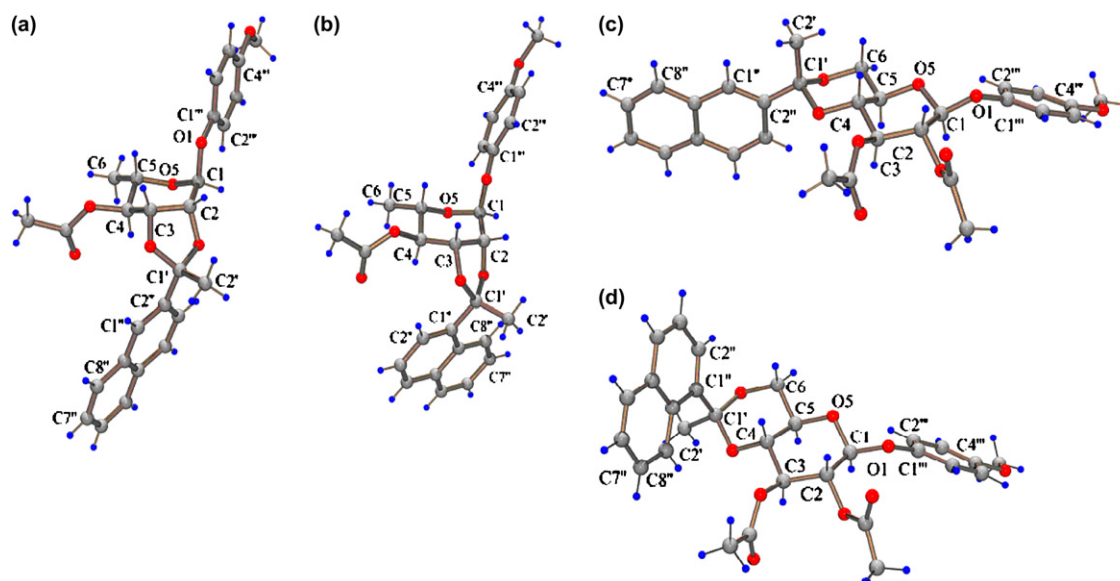

Figure 3. DeVoe calculations of (1'R)-3 and (1'R)-5 using the X-ray geometries as input.

(1'R)-5 were measured with the KCl pellet technique, to be correlated with the solid-state X-ray structures and the solution CDs. Since the results of DeVoe-type calculations using MMFF or X-ray geometries proved that the X-ray structures of (1'R)-3 and (1'R)-5 were also dominant and/or determined the CD properties in solution, solid-state CDs were expected to be similar to the solution ones if intermolecular coupling interactions do not have a significant contribution.[23] In accordance, the solid-state CDs of (1'R)- and (1'S)-3 were almost identical with the solution ones supporting the view of a prevalent intramolecular origin of the solid-state CD (Fig. 1c and Table 1). In contrast, in the solid-state CD of (1'R)-5, all of the CEs were reversed compared to its solution spectrum; their magnitudes were markedly increased and a strong negative couplet appeared in the naphthyl ^1B_b/phenyl ^1L_a region [233 nm (−107.2), 216 nm (62.3)]. Based on CD and MMFF calculations, the observed solid-state CD of (1'R)-5 could not be due to conformational differences between the solution and
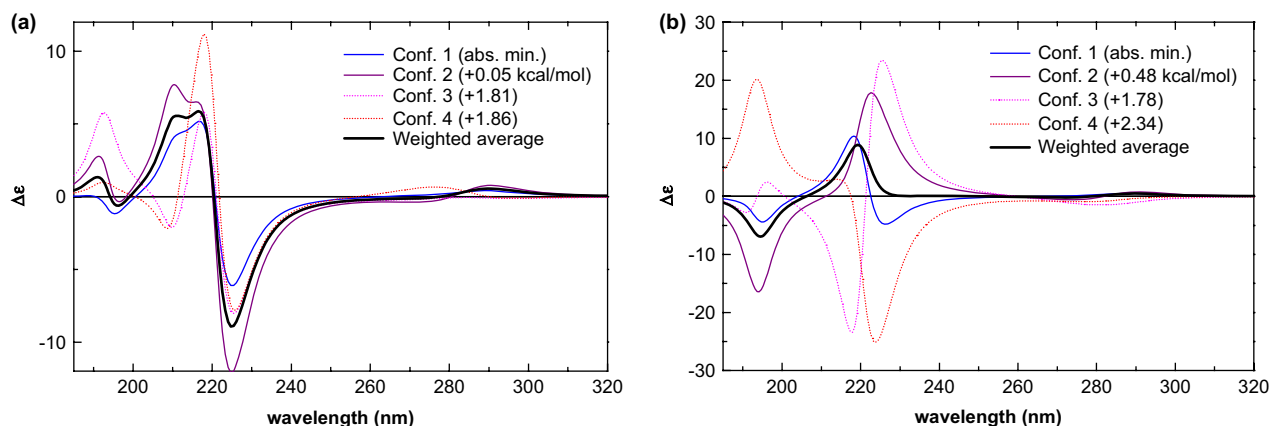

Figure 2. ORTEP structures of (a) (1'R)-3, (b) (1'R)-5, (c) (1'R)-11, and (d) (1'S)-12a.

Figure 4. DeVoe calculations of (1′R)-**3** (a) and (1′R)-**5** (b) using MMFF geometries.

solid-state geometries, and it could not be of only intramolecular origin. In order to shed light on this solid-state CD, the relative arrangement of the aromatic naphthyl and DMB chromophores from different molecules were checked in the crystal lattice from the X-ray analysis of (1′R)-**5** (Fig. 5). The X-ray data clearly showed that the naphthyl groups of different (1′R)-**5** molecules are not stacked and neighboring naphthyl groups are tilted relative to one another. With this orientation an intermolecular coupling is feasible between neighboring naphthyl and anisole chromophores. The sign and intensity of the ECCD interaction between two chromophores can be estimated on the basis of the projection angle θ (looked through the centers) and the center-to-center distance r (Fig. 2).[11,12] A positive acute projection angle θ is associated with a positive couplet; the maximum ECCD intensity is observed for $\theta \approx \pm 70°$, while $\theta \approx 0°$ and $180°$ lead to negligible ECCD. In addition, the exciton coupling strength varies with the inverse third power of distance, r^{-3}. Within a threshold center-to-center distance of 10 Å, each naphthyl in the crystal lattice of (1′R)-**5** is surrounded by three other naphthyls and

two DMB groups. Some of the intermolecular naphthyl–naphthyl distances are even shorter than the intramolecular separation of linked naphthyl and DMB moieties, which is 7.0 Å for the C-1″–C-1′ distance, and 9.4 Å for the center-to-center distance. The naphthyl group denoted with letter A in Figure 5, taken as a probe, has two nearby naphthyls (B and C) with center-to-center distances r_{AB} and r_{AC}=7.0 Å, plus a third naphthyl (D) at r_{AD}=9.4 Å. The relative alignment of naphthyls B–D with A allows for a strong exciton interaction of their long-axis polarized transitions. The projection angles between the long axes of naphthyls A and B/C are $\theta_{A,B}$ and $\theta_{A,C}$=−37.8°, both associated with negative ECCD. The same is true for the A/D coupling, having $\theta_{A,D}$=−66.0°. The dimethoxybenzene moiety E is the closest interacting chromophore to naphthyl A, with a distance r_{AE}=5.4 Å and a projection angle $\theta_{A,E}$=+45.0° between the long axes, which should lead to a moderate positive ECCD. A second DMB (F) lies at distance r_{AF}=7.3 Å with projection angle $\theta_{A,F}$=−45.0°.

To support the expectations for intermolecular couplings in the lattice, DeVoe calculations were performed to ascertain the coupling interactions of the naphthyl and DMB moieties of the probe molecule with the respective surrounding chromophores. Three interacting naphthyls (B, C, D) and two DMB's (E and F) were taken into account for the probe naphthyl (A), and four naphthyls and one DMB (not indicated) for the probe DMB (A′). The DeVoe-calculated CD (Fig. 6) consists of a strong negative ECCD for the naphthyl-centered system and small positive one for the DMB-centered one around 220 nm. Provided that these interactions are additive,[12] the CDs of the two systems can be added to produce a strong negative couplet for the overall interchromophoric interaction sensed by each (1′R)-**5** molecule in the lattice. It must, however, be stressed that DeVoe calculations on compounds containing multiple naphthalene units tend to overestimate degenerate naphthyl–naphthyl coupling terms in comparison with nondegenerate couplings between naphthyls and other chromophores;[15a] therefore, the intensity of the negative couplet in Figure 6 is probably exaggerated.

This result confirms that, rather than the intramolecular naphthyl–DMB coupling, it is the intermolecular naphthyl–naphthyl interaction that dominates the solid-state CD of
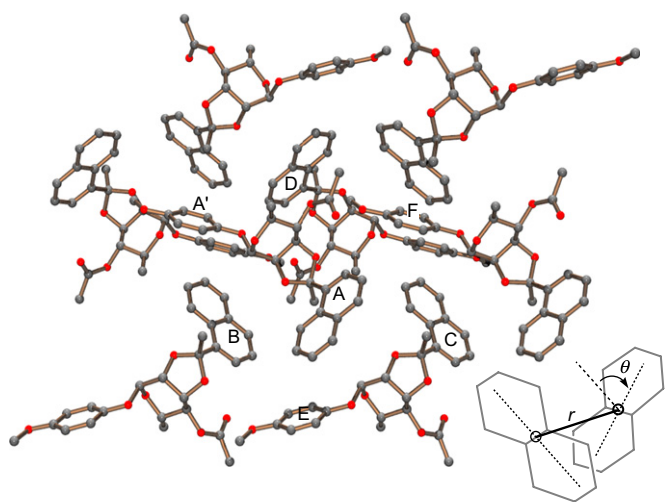

Figure 5. Orientation of the neighboring molecules of (1′R)-**5** in the solid state emphasizing the intermolecular exciton-coupled interactions of the aromatic chromophores, and definition of the projection angle for two long-axis polarized naphthyl transitions.
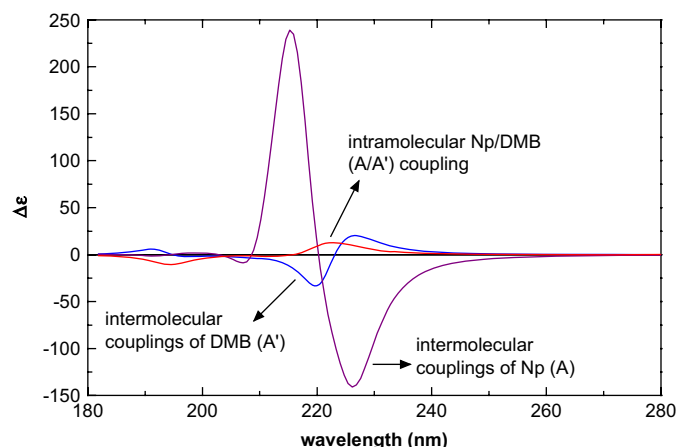
Figure 6. DeVoe calculations of the couplings between the probe naphthyl (Np) and DMB chromophores (A and A′ in Fig. 5) with the closest, strong interacting chromophores in (1′R)-5 crystals. For Np A, three Np's and two DMB's were included; for DMB A′, four Np's and one DMB were included. To compare with the intramolecular coupling between A and A′ (also shown), spectra are scaled to the number of coupling chromophores (five for both A and A′).

(1′R)-5. In solution, the regular arrangement of the chromophores is disrupted and hence only the intramolecular naphthyl–DMB interaction is measured. The present correlation of the solid-state and solution CD, X-ray analysis, and CD calculation of (1′R)-5 provides a rare example demonstrating the presence of intermolecular ECCD interactions in the solid-state, and allowing the difference between the solution and solid-state CD to be interpreted.

The X-ray analysis of (1′R)-3 also explains the similarity of its solution and solid-state CD spectra (Fig. 7). In the single crystal, every two proximal molecules of (1′R)-3 are closely stacked in a head-to-head and tail-to-tail fashion, namely two naphthyls are stacked somewhat displaced and two anisoles are stacked aligned. Due to such an orientation, no ECCD is possible between the stacking chromophores, since the projection angles of their long-axis transitions are 0° or 180°. Distinct stacking pairs of the same chromophore are arranged parallel on top of one another somewhat rotated, but the projection angles are again close to 0° or 180°. Since the intramolecular interactions remain the strongest in the single crystal, the solid-state CD is quite similar to the solution one. DeVoe calculations on lattice structure of (1′R)-3 confirmed that the couplings between stacked naphthyls are null, while those between the probe naphthyl and surrounding non-stacked naphthyls give a positive couplet [231 (+19.5), 211 (−21.2)]. Its intensity (scaled to four couplings) is one order of magnitude smaller than that calculated for (1′R)-5 lattice. The comparison with the computed naphthyl–DMB intramolecular coupling in (1′R)-3 (Fig. 3) is biased in favor of the naphthyl–naphthyl couplings, as discussed above. However, the overall result is in full accordance with the view that intermolecular exciton couplings in the crystals play a decisive role in the solid-state CD of (1′R)-5 but not in that of (1′R)-3.

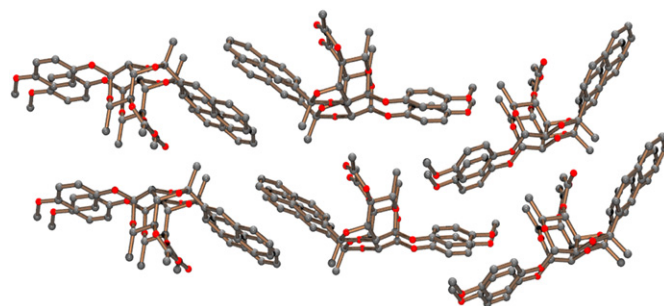For the preparation of 1,3-dioxane-type naphthylethylidene ketals, p-methoxyphenyl β-D-glucopyranoside 10 was selected

Figure 7. Orientation of the neighboring molecules of (1′R)-3 in the solid-state. The naphthyl and DMB moieties of two aligned molecules are stacked closely and the stacking pairs of the same kind are also arranged on the top of one another.

as starting material (Scheme 2), since the products (1′R)-11 and 12 could be compared with the analogous (2-naphthyl)-methylene acetal 13 published earlier (Fig. 8).[6]
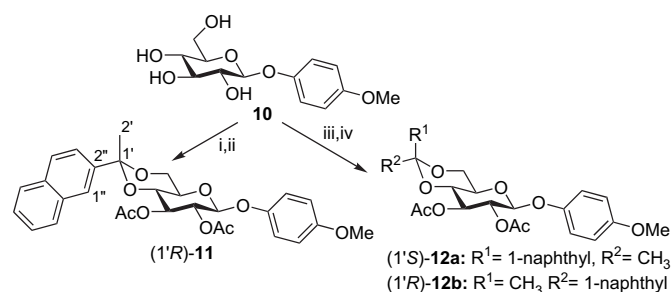
Scheme 2. (i) 6, (+)-10-CSA, dry DMF. (ii) Ac$_2$O/dry pyr. (iii) 7, PTS, dry DMF. (iv) Ac$_2$O/dry pyr.

The reaction of 10 with 6 in the presence of (+)-10-camphorsulfonic acid provided the (2-naphthyl)ethylidene ketal (1′R)-11 in moderate yield. The CD spectrum of (1′R)-11 could be compared with that of its deacetylated (2-naphthyl)methylene ketal analogue 13 in which the equatorial arrangement of the 2-naphthyl group had been unambiguously determined (Fig. 8).[6] Since both (1′R)-11 and 13 gave a positive CE at 225 nm and a negative one at 194 nm due to the interaction of naphthyl ^1B_b and phenyl ^1B transitions, their CD data suggested that the naphthyl group of (1′R)-11 was also oriented equatorially, which was also confirmed by its X-ray analysis (Fig. 1d).

The X-ray data also revealed that the 2-naphthyl group has an equatorial parallel conformation with the torsional angle $\omega_{C-2',C-1',C-2'',C-1''} = -7.3°$. An MMFF conformational analysis of (1′R)-11 revealed instead that all the calculated low-energy conformers have a perpendicular orientation of the naphthyl ring with respect to methyl group ($\omega_{C-2',C-1',C-2'',C-1''} \approx \pm 90°$). By means of torsional energy scans, the parallel orientation was estimated to have a much higher energy than the perpendicular one, by 2.20 kcal/mol (MMFF) or 1.40 kcal/mol (semi-empirical AM1). The unfavorable parallel orientation of the naphthyl group may have been induced during the crystallization to produce a closely stacked head-to-head/tail-to-tail pair in the single crystal, similar to that of (1′R)-3. Similar to (1′R)-3, no ECCD is possible within each stacking pair,
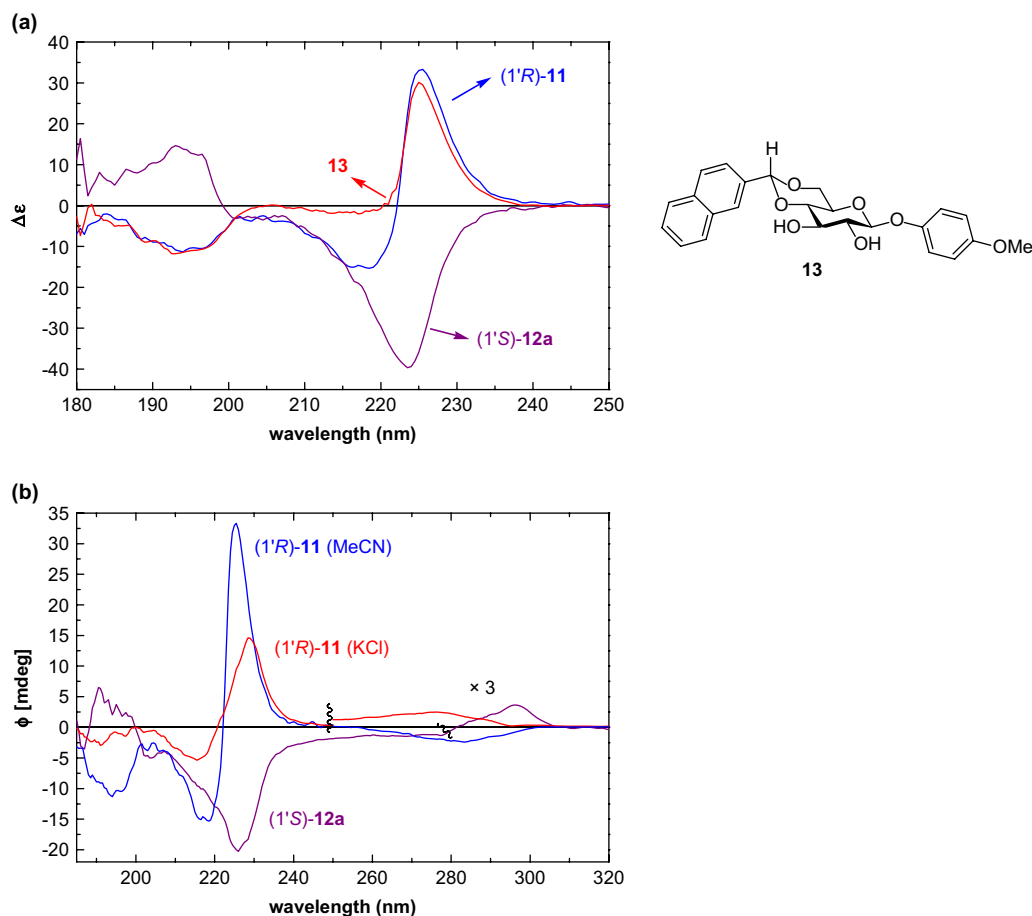
Figure 8. (a) CD spectra of compounds (1′R)-**11**, (1′S)-**12a**, and **13** in acetonitrile. (b) CD spectra of (1′R)-**11** and (1′S)-**12a** in KCl and solution CD of (1′R)-**11**.

and only very weak ones are possible between distinct pairs, since the projection angles of the long-axis polarized naphthyl transitions were close to 0° or 180°. It is also noteworthy that in contrast to (1′R)-**3**, the planes of the distinct stacking pairs of the same chromophores are arranged alternately orthogonal on top of one another. Thus the solid-state CD should be mainly of intramolecular origin and derive from a different conformer than that predominant in solution. In addition to the different orientation of the naphthyl ring, the solid-state structure of (1′R)-**11** shows a second torsion $\omega_{C-1''',O-1,C-1,H-1} =$ 27°, far from the MMFF geometries where it is $\approx \pm 60°$. In practice, the overall arrangement between the exciton-coupled naphthyl and DMB chromophores differs a lot between solid-state and lowest energy MMFF-computed structures of (1′R)-**11**. In agreement with these findings, in the solid-state CD of (1′R)-**11** (Fig. 8b), the naphthyl ^1L_a band showed a positive CE at 277 nm compared to the negative solution one [283 nm (−4.4)]. Minor differences are also seen in the shape and cross-over points of the positive CD couplet around 220 nm: in fact, the two couplets are of different origin. The strong positive CD couplet in solution is due to the coupling between naphthyl ^1B_b and phenyl $^1L_a/^1B_a$ transitions, as deduced from DeVoe calculations on the four low-energy MMFF-calculated conformers, differing in the torsions $\omega_{C-2',C-1',C-2'',C-1''} \approx \pm 90°$ and $\omega_{C-1''',O-1,C-1,H-1} \approx \pm 60°$ (Fig. 10a). In the solid-state, the coupling of naphthyl ^1B_b with long-axis

polarized phenyl transitions is less effective due to the different conformation as discussed above. DeVoe calculations on the X-ray structure (Fig. 9) show that the less intense naphthyl ^1B_a transition (short-axis polarized) brings about the stronger contribution to the moderate positive couplet as found in the corresponding experimental CD.

The reaction of **10** with **7** in the presence of PTS afforded a mixture of the axial and equatorial 1-naphthyl ketals, which
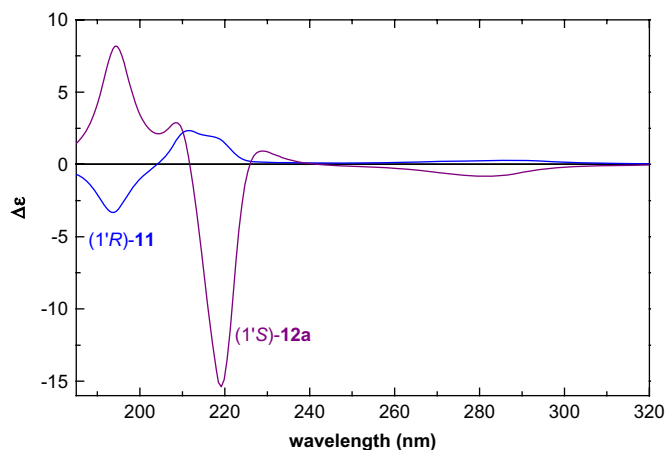

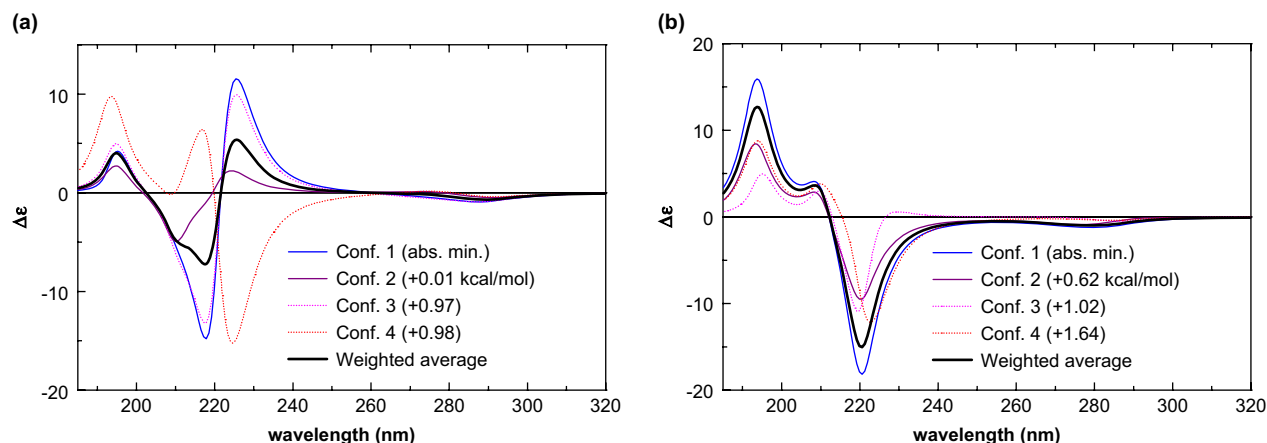Figure 9. DeVoe calculations of (1′R)-**11** and (1′S)-**12a** using the X-ray geometries as input.

Figure 10. DeVoe calculations of (1′R)-**11** (a) and (1′S)-**12a** (b) using MMFF geometries.

could be separated after acetylation as (1′S)-**12a** and (1′R)-**12b**, respectively (Scheme 2). Due to steric crowding, (1′R)-**12b** was quite unstable and it was slowly decomposing in solution and partially rearranging to the thermodynamically more stable axial ketal (1′S)-**12a**. Thus the stereochemical study was focused on (1′S)-**12a**, the single crystals of which could be produced in hexane/ethyl acetate 10:1 for X-ray analysis (Fig. 2d). The X-ray data showed that its 1-naphthyl group has an axial orientation with torsional angle $\omega_{\text{C-2}',\text{C-1}',\text{C-1}'',\text{C-2}''}=$ 102.4°, which implies a near perpendicular conformation of the naphthyl with respect to the methyl group. A similar conformer was also found as the most stable one by a MMFF conformational search. As in the other cases above, three other low-energy MMFF conformers were also taken in to account, differing in the torsions $\omega_{\text{C-2}',\text{C-1}',\text{C-1}'',\text{C-2}''} \approx \pm 90°$ and $\omega_{\text{C-1}''',\text{O-1},\text{C-1},\text{H-1}} \approx \pm 60°$. The DeVoe-calculated CDs of the individual conformers and their averaged spectrum (Fig. 10b) reproduced the strong negative CD couplet (Table 1 and Fig. 8) that derives from the coupling between the naphthyl ^1B_b and phenyl $^1B_{a,b}$ transitions. On the contrary, the positive CD sign of naphthyl ^1L_a transition [293 (1.3), 283sh (0.9), 272sh (0.1)] was not predicted by the DeVoe method, probably due to its non-excitonic origin. The solid-state CD spectrum of (1′S)-**12a** was quite similar to the solution one; a negative CD couplet below 240 nm and a positive naphthyl ^1L_a band were measured (Table 1 and Fig. 8). A DeVoe calculation on the X-ray geometry (Fig. 9) reproduced again the experimental solid-state CD except for the sign of naphthyl ^1L_a band. The similarity of the solution and solid-state CDs, as well as the CD calculation results, demonstrate that the solid-state CD of (1′S)-**12a** is mainly determined by the same intramolecular effects that are prevalent in solution. This is further supported by the structural similarity between the solid-state geometry and the lowest energy MMFF conformer.

3. Conclusion

Solution and solid-state circular dichroism, X-ray diffraction, and DeVoe-type CD calculations on the solid-state geometry and on the calculated MMFF conformers of (1′R)-**3**, (1′R)-**5**, (1′R)-**11**, and (1′S)-**12a** allowed us to interpret the observed exciton-coupled interactions and to determine the conformers in solution and in the solid state. For (1′R)-**3** and (1′S)-**12a**, nearly identical solution and solid-state CDs were measured, which implies that the conformations found in their X-ray structures are also prevalent in solution. This hypothesis was further confirmed by DeVoe CD calculations on their X-ray and MMFF-calculated geometries, which reproduced the solid-state and solution CDs, respectively. The study of their X-ray clusters also showed that no significant intermolecular ECCD can be expected between the stacking molecules or the stacking pairs. In contrast, the solution and solid-state CDs of (1′R)-**5** were very different and the CD calculations proved that this difference cannot be derived from different conformations in solution and solid state, but instead is due to intermolecular ECCDs between neighboring aromatic chromophores in the solid state. In the crystal lattice of (1′R)-**5**, intermolecular exciton couplings are responsible for intense ECCD that may override the intramolecular one. A DeVoe calculation of a solid-state cluster extracted from the X-ray data reproduced the large negative exciton couplet of (1′R)-**5**. This example emphasizes that the intermolecular ECCD of strong aromatic chromophores have to be considered as a possible reason for differences between solid-state and solution CDs. Moreover, it also provides a rare example of recognition of intermolecular ECCD interactions in the solid state. (1′R)-**11** has different conformations in solution and solid state but except for the naphthyl ^1L_a band, the solution and solid-state CD spectra had only subtle differences, both having a positive ECCD below 240 nm. However, the CD calculations confirmed that the positive exciton couplets in solution and solid state derived from different mechanisms, i.e., the coupling of different naphthyl electric transition moments with the long-axis polarized phenyl transitions.

4. Experimental

4.1. General

Melting points were determined on a Kofler hot-stage apparatus and are uncorrected. The NMR spectra were recorded on Bruker-AMX 500 (^{1}H: 500 MHz; ^{13}C: 125 MHz), Bruker WP

200 SY (^{1}H: 200 MHz, ^{13}C: 50 MHz), and Bruker Aspect 3000 (^{1}H: 360 MHz) spectrometers using TMS as internal standard. Chemical shifts were reported in parts per million. Optical rotation were determined with a Perkin–Elmer 241 polarimeter. CD spectra were recorded on a J-810 spectropolarimeter. The CD spectra were measured in millidegrees and normalized into $\Delta\varepsilon_{max}$ [l mol^{-1} cm^{-1}]/λ [nm] units. For solid-state CD protocol, see Refs. 16–22. IR spectra were recorded on an Perkin–Elmer 16 PC FTIR spectrometer and absorption bands presented in cm^{-1}. Precoated silica gel plates (Kieselgel 60 F$_{254}$, 0.25 mm, Merck) were used for analytical and preparative TLC. High resolution FAB mass spectra were measured on a JEOL JMS-DX303 HF mass spectrometer using a glycerol matrix and Xe ionizing gas and ESI-TOF MS measurements were performed on a MicroTOF-Q instrument (Bruker Daltonik GmbH, Bremen, Germany).

4.2. X-ray crystallography

Data were collected at 293(1) K, Enraf Nonius MACH3 diffractometer, Mo Kα radiation $\lambda=0.71073$ Å, ω motion. Raw data were evaluated using the XCAD4[24] or the PROFIT[25] software, the structure was solved using direct methods by SIR-92[26] and refined on F^2 using SHELX-97[27] program. Refinement was performed anisotropically for non-hydrogen atoms. Hydrogen atoms were placed into geometric position. Publication material was prepared with the WINGX-97 suite.[28] The ORTEP[29] and PLATON programs[30] were used for crystallographic calculations. Except for (1′R)-5, the crystals were rather weakly diffracting ones, resulting in low

percentage of observed reflections and high but acceptable R factors of around 9%. However, bond length and bond angle data are reasonable and the overall error can be attributed to the generally low quality of the crystals (Table 2). Full crystallographic data (excluding structure factors) of (1′R)-3, (1′R)-5, 11, and (1′S)-12a have been deposited with the Cambridge Crystallographic Data Centre as supplementary publication no. CCDC 660892–660895. Copies of the data can be obtained free of charge on application to CCDC, 12 Union Road, Cambridge CB2 1EZ, UK (fax: +44 1223 336 033; e-mail: deposit@ccdc.cam.ac.uk).

4.2.1. (1′R)-p-Methoxyphenyl 6-deoxy-2,3-O-(1-naphthy)-ethylidene-α-L-rhamnopyranoside [(1′R)-2] and (1′S)-p-methoxyphenyl 6-deoxy-2,3-O-(1-naphthy)ethylidene-α-L-rhamnopyranoside [(1′S)-2]

To a suspension of **1** (201.6 mg, 0.75 mmol) in CH$_3$CN (5 ml), 1-(1,1-dimethoxyethyl)naphthalene (**6**) (915 mg, 4.24 mmol) and a catalytic amount of (+)-10-camphorsulfonic acid (98.3 mg, 0.393 mmol) were added, and the mixture was stirred at room temperature for 2.5 h. Dichloromethane (10 ml) was added to the mixture and washed with saturated aqueous solution of Na$_2$CO$_3$ and brine. The combined organic layer was dried on Na$_2$SO$_4$, filtered, and concentrated to give a foam (264 mg, 84%). For the spectroscopic characterization, 100 mg were purified by preparative TLC (hexane/ethyl acetate=4:1), which afforded 90% (1′R)-2 and 10% (1′S)-2 as isolated yields.

(1′R)-2: ^{1}H NMR (200 MHz, CDCl$_3$) δ 7.98–7.39 (m, 7H, H-naphthyl), 6.97–6.75 (m, 4H, H-phenyl), 5.70 (s, 1H, H-1),

Table 2
Crystallographic data of (1′R)-3, (1′R)-5, (1′R)-11, and (1′S)-12a

Ref. No.	(1′R)-3	(1′R)-5	(1′R)-11	(1′S)-12a
Empirical formula	C$_{27}$H$_{28}$O$_7$	C$_{27}$H$_{28}$O$_7$	C$_{29}$H$_{30}$O$_9$	C$_{29}$H$_{30}$O$_9$
Formula weight	464.49	464.49	522.53	522.53
Crystal system	Orthorhombic	Orthorhombic	Monoclinic	Monoclinic
Space group	$P2_12_12_1$ (no. 19)	$P2_12_12_1$ (no. 19)	$P2_1$ (no. 4)	$P2_1$ (no. 4)
a (Å)	6.1398(10)	12.0219(10)	5.6715(10)	13.812(4)
b (Å)	7.684(2)	12.492(2)	8.4110(10)	6.413(7)
c (Å)	50.5601(10)	15.6533(10)	27.6179(10)	15.666(6)
β (°)	90	90	91.90(1)	97.43(3)
V (Å^3)	2385.4(7)	2350.8(4)	1316.7(3)	1376.0(16)
Z	4	4	2	2
Dimensions of crystal (mm)	0.36/0.25/0.2	0.36/0.25/0.2	0.35/0.2/0.15	0.56/0.03/0.02
Crystal color and habit	Colorless block	Colorless block	Colorless prism	Colorless needle
D_{calcd} (g cm^{-3})	1.293	1.312	1.318	1.261
μ (Mo Kα)/mm^{-1}	0.09	0.10	0.10	0.09
θ_{max} (°)	25.3	26.0	25.5	25.3
No. observed reflections [$I>2.00\sigma(I)$]	2099	1456	811	1048
No. independent reflections	2945	2585	2192	2954
No. variables	307	307	343	343
Residuals: $R_1(F)/wR_2(F^2)^a$	0.090/0.243	0.056/0.219	0.094/0.216	0.086/0.239
Goodness of fit	1.29	0.86	0.90	1.36
Max./Min. peak in final difference map/e Å^{-3}	0.35/−0.34	0.25/−0.23	0.24/−0.25	0.35/−0.32

^{a} $R_1(F) = \sum(|F_0| - |F_c|)/\sum(|F_0|)$; $wR_2(F^2) = [\sum w(|F_0^2| - |F_c^2|)^2 / \sum w(|F_0^2|)^2]^{1/2}$.

4.48 (d, 1H, J=5.3 Hz, H-2), 4.34 (dd, 1H, J=7.6, 5.3 Hz, H-3), 3.70 (s, 3H, OMe), 3.70–3.60 (m, 1H, H-5), 3.06 (dd, 1H, J=9.8, 7.6 Hz, H-4), 1.94 (s, 1H, OH), 1.66 (s, 3H, acetal Me), 0.95 (d, 3H, J=6.2 Hz, C-5 Me); ^{13}C NMR (50 MHz, CDCl$_3$, 25 °C) δ 155.0 (C-q phenyl), 150.2 (C-q phenyl), 141.6 (C-q naphthyl), 132.9 (2×C-q naphthyl), 128.4–123.2 (7×C-t naphthyl), 117.8 (2×C-t phenyl), 114.6 (2×C-t phenyl), 109.8 (C acetal), 96.2 (C-1), 79.2–72.7 (C-2 to C-4), 66.4 (C-5), 55.6 (OMe), 28.9 (Me), 17.1 (C-6). Calcd for [M+Na]$^+$ 445.162, found mass for C$_{27}$H$_{28}$O$_7$ [M+Na]$^+$ 445.162.

(1′S)-**2**: [α]$_D$ +18.9 (*c* 0.1, CHCl$_3$), ^{1}H NMR (200 MHz, CDCl$_3$) δ 7.99–7.47 (m, 7H, H-naphthyl), 6.97–6.78 (m, 4H, H-phenyl), 5.68 (s, 1H, H-1), 4.32 (t, 1H, J=6.4 Hz), 4.07 (d, 1H, J=6.4 Hz, H-2), 3.90–3.60 (m, 2H), 3.76 (s, 3H, OMe), 1.85 (s, 3H, acetal Me), 1.70 (s, 1H, OH), 1.31 (d, 3H, J=6.2 Hz, C-5 Me); ^{13}C NMR (125 MHz, CDCl$_3$, 25 °C) δ 154.9 (C-q phenyl), 150.1 (C-q phenyl), 140.8 (C-q naphthyl), 133.0 (C-q naphthyl), 132.8 (C-q naphthyl), 130.9–123.3 (7×C-t naphthyl), 117.5 (2×C-t phenyl), 114.5 (2×C-t phenyl), 109.8 (C acetal), 96.1 (C-1), 78.4–75.2 (C-2 to C-4), 66.6 (C-5), 55.6 (OMe), 29.2 (Me), 17.5 (C-6). Calcd for [M+Na]$^+$ 445.162, found mass for C$_{27}$H$_{28}$O$_7$ [M+Na]$^+$ 445.163.

4.2.2. (1′R)-p-Methoxyphenyl 4-O-acetyl-6-deoxy-2,3-O-(2-naphthyl)ethylidene-α-L-rhamnopyranoside [(1′R)-3] and (1′S)-p-methoxyphenyl 4-O-acetyl-6-deoxy-2,3-O-(2-naphthyl)ethylidene-α-L-rhamnopyranoside [(1′S)-3]

The 9:1 mixture of (1′R)-**2** and (1′S)-**2** (158 mg, 0.374 mmol) was treated with pyridine (1.5 ml) and acetic anhydride (1.5 ml) for 12 h at room temperature. Then the solution was slowly quenched with aqueous 10% HCl and extracted with ethyl acetate (3×10 ml). The organic layer was washed with saturated aqueous solution of NaHCO$_3$ (3×) and brine, dried (MgSO$_4$), filtered, and concentrated in vacuum to give a yellow oil (221 mg, 85%). The (1′R)-**3** isomer was crystallized from hexane (mp: 111–112 °C), and the residue was purified further by preparative TLC (hexane/ethyl acetate=3:1) to give (1′S)-**3**, mp: 131–133 °C.

(1′R)-**3**: [α]$_D$ −91.9 (*c* 0.8, CHCl$_3$); IR ν_{max} (KBr) 2932, 1742, 1592, 1508, 1376, 1284, 1230, 1138, 1038, 826, 748 cm^{-1}; ^{1}H NMR (500 MHz, CDCl$_3$) δ 8.05–7.46 (m, 7H, H-naphthyl), 6.84 (dd, 2H, J=8.8, <1 Hz, H-arom.), 6.82 (dd, 2H, J=8.8, <1 Hz, H-arom.), 5.73 (s, 1H, H-1), 4.64 (m, 2H, H-2+H-3), 4.59 (m, 1H, H-4), 3.84 (m, 1H, H-5), 3.56 (s, 3H, OMe), 2.08 (s, 3H, OAc), 1.73 (s, 3H, acetal Me), 0.93 (d, 3H, J=6.2 Hz, C-5 Me); ^{13}C NMR (125 MHz, CDCl$_3$, 25 °C) δ 169.3 (C acetyl), 155.1 (C-q phenyl), 150.2 (C-q phenyl), 140.3 (C-q naphthyl), 133.1 (C-q naphthyl), 132.9 (C-q naphthyl), 128.6–123.4 (7×C-t naphthyl), 117.7 (2×C-t phenyl), 114.7 (2×C-t phenyl), 110.4 (C acetal), 96.1 (C-1), 76.6–73.5 (C-2 to C-4), 64.8 (C-5), 55.6 (OMe), 28.6 (Me), 20.9 (acetyl), 16.9 (C-6). Calcd for [M+Na]$^+$ 487.173, found mass for C$_{27}$H$_{28}$O$_7$ [M+Na]$^+$ 487.174.

(1′S)-**3**: [α]$_D$ −25.8 (*c* 1.0, CHCl$_3$); IR ν_{max} (KBr) 2934, 1740, 1570, 1508, 1378, 1224, 1138, 1106, 1040, 768 cm^{-1};

^{1}H NMR (500 MHz, CDCl$_3$) δ 7.97–7.48 (m, 7H, H-naphthyl), 6.94 (dd, 2H, J=9.3, <1 Hz, H-arom.), 6.80 (dd, 2H, J=9.3, <1 Hz, H-arom.), 5.70 (s, 1H, H-1), 5.09 (dd, 1H, J=9.9, 7.5 Hz, H-4), 4.42 (dd, 1H, J=7.5, 5.5 Hz, H-3), 4.09 (d, 1H, J=6 Hz, H-2), 3.93 (m, 1H, H-5), 3.75 (s, 3H, OMe), 2.18 (s, 3H, OAc), 1.89 (s, 3H, acetal Me), 1.12 (d, 3H, J=6.4 Hz, C-5 Me); ^{13}C NMR (125 MHz, CDCl$_3$, 25 °C) δ 170.2 (C acetyl), 155.0 (C-q phenyl), 150.2 (C-q phenyl), 140.9 (C-q naphthyl), 133.0–132.8 (C-q naphthyl), 128.3–123.4 (7×C-t naphthyl), 117.5 (2×C-t phenyl), 114.6 (2×C-t phenyl), 110.0 (C acetal), 96.0 (C-1), 76.0 (C-2, C-3), 74.9 (C-4), 64.9 (C-5), 55.6 (OMe), 28.9 (Me), 21.1 (acetyl), 17.1 (C-6). Calcd for [M+Na]$^+$ 487.173, found mass for C$_{27}$H$_{28}$O$_7$ [M+Na]$^+$ 487.175.

4.2.3. (1′R)-p-Methoxyphenyl 6-deoxy-2,3-O-(1-naphthyl)-ethylidene-α-L-rhamnopyranoside [(1′R)-4]

To a suspension of **1** (300 mg, 1.11 mmol) in CH$_3$CN (10 ml), 1-(1,1-dimethoxyethyl)naphthalene (**7**) (480 mg, 2.22 mmol) and a catalytic amount of p-toluenesulfonic acid (10 mg, 0.053 mmol) were added and the mixture was stirred at room temperature for 5 h. Then the mixture was neutralized with triethylamine and evaporated in vacuum. The residue was purified by column chromatography (hexane/ethyl acetate=9:1) to give a foam (419 mg, 89%). [α]$_D$ −74.9 (*c* 0.9, CHCl$_3$); ^{1}H NMR (200 MHz, CDCl$_3$) δ 8.57 (d, 1H, J=9.3 Hz, H-naphthyl), 7.92–7.42 (m, 6H, H-naphthyl), 7.05–6.82 (m, 4H, H-phenyl), 5.78 (s, 1H, H-1), 4.60 (d, 1H, J=5.3 Hz, H-2), 4.46 (dd, 1H, J=7.6, 5.3 Hz, H-3), 3.78 (s, 3H, OMe), 3.77–3.71 (m, 1H, H-5), 3.12 (dd, 1H, J=9.8, 7.6 Hz, H-4), 1.88 (s, 1H, OH), 1.87 (s, 3H, acetal Me), 1.01 (d, 3H, J=6.2 Hz, C-5 Me); ^{13}C NMR (125 MHz, CDCl$_3$, 25 °C) δ 155.0 (C-q phenyl), 150.3 (C-q phenyl), 140.2 (C-q naphthyl), 134.4 (C-q naphthyl), 129.8 (C-q naphthyl), 129.0–122.6 (C-t naphthyl), 117.8 (C-t phenyl), 114.6 (C-t phenyl), 110.5 (C acetal), 96.3 (C-1), 79.1–66.3 (C-2 to C-5), 55.6 (OMe), 29.0 (Me), 16.9 (C-6). Calcd for [M+Na]$^+$ 445.162, found mass for C$_{27}$H$_{28}$O$_7$ [M+Na]$^+$ 445.163.

4.2.4. (1′R)-p-Methoxyphenyl 4-O-acetyl-6-deoxy-2,3-O-(1-naphthyl)ethylidene-α-L-rhamnopyranoside [(1′R)-5]

(1′R)-**4** (88 mg, 0.208 mmol) was treated with pyridine (0.5 ml) and acetic anhydride (0.5 ml) for 12 h at room temperature. Then the solution was slowly quenched with aqueous 10% HCl and extracted with ethyl acetate (3×10 ml). The organic layer was washed with saturated aqueous solution of NaHCO$_3$ (3×) and brine, dried (MgSO$_4$), filtered, and concentrated in vacuum to give a foam (94 mg, 93%), which was crystallized from hexane. Mp: 144–145 °C; [α]$_D$ −82.2 (*c* 0.9, CHCl$_3$); IR ν_{max} (KBr) 2932, 1744, 1508, 1370, 1288, 1228, 1128, 1102, 1038, 826, 780 cm^{-1}; ^{1}H NMR (500 MHz, CDCl$_3$) δ 8.51–7.47 (m, 7H, H-naphthyl), 7.02 (dd, 2H, J=9.2, <1 Hz, H-arom.), 6.84 (dd, 2H, J=9.2, <1 Hz, H-arom.), 4.66–4.64 (m, 2H, H-2+H-3), 4.62 (m, 1H, H-4), 3.85 (m, 1H, H-5), 3.78 (s, 3H, OMe), 2.04 (s, 3H, OAc), 1.89 (s, 3H, acetal Me), 0.93 (d, 3H, J=6.2 Hz,

C-5 Me); ^{13}C NMR (125 MHz, CDCl$_3$, 25 °C) δ 169.1 (C acetyl), 155.0 (C-q phenyl), 150.2 (C-q phenyl), 139.0 (C-q naphthyl), 134.3 (C-q naphthyl), 129.9 (C-q naphthyl), 129.1–123.2 (7×C-t naphthyl), 117.7 (2×C-t phenyl), 114.6 (2×C-t phenyl), 110.9 (C acetal), 96.1 (C-1), 76.2–75.8 (C-2, C-3), 73.2 (C-4), 64.9 (C-5), 55.6 (OMe), 28.6 (Me), 20.7 (C acetyl), 16.8 (C-6). Calcd for [M+Na]$^+$ 487.173, found mass for C$_{27}$H$_{28}$O$_7$ [M+Na]$^+$ 487.175.

4.2.5. (1′S)-p-Methoxyphenyl 2,3-O-(2-naphthyl)methylene-α-L-rhamnopyranoside and (1′R)-p-methoxyphenyl 2,3-O-(2-naphthyl)methylene-α-L-rhamnopyranoside [deacetylated derivatives of (1′S)-9 and (1′R)-9]

To a solution of p-methoxyphenyl α-L-rhamnopyranoside (1) (4.045 g, 15 mmol) in DMF (10 ml), 2-(dimethoxymethyl)naphthalene (4.7 ml, 23 mmol, 1.55 equiv) and p-toluenesulfonic acid (220 mg) were added and the mixture was stirred for 90 h at room temperature, when the conversion reached 90% (TLC: hexane/ethyl acetate=7:3). The solution was diluted with dichloromethane (DCM) (200 ml) and was extracted once with aq NaHCO$_3$ (50 ml) and with water (3×30 ml). The united aqueous phases were extracted once more with DCM, and the united organic layers were dried over MgSO$_4$, filtered and evaporated in vacuum. The syrupy residue was purified by column chromatography using hexane/ethyl acetate=8:2+5% triethylamine (TEA) as the eluent. Yield of 4.768 g (78%) was directly used for the next step.

4.2.6. (1′S)-p-Methoxyphenyl 4-O-acetyl-2,3-O-(2-naphthyl)methylene-α-L-rhamnopyranoside [(1′S)-9] and (1′R)-p-methoxyphenyl 4-O-acetyl-2,3-O-(2-naphthyl)-methylene-α-L-rhamnopyranoside [(1′R)-9]

p-Methoxyphenyl 2,3-O-(2-naphthyl)methylene-α-L-rhamnopyranoside [(1′S) and (1′R)] (1.606 g, 3.9 mmol) was dissolved in pyridine (4 ml) and acetic anhydride (3 ml) was added and the solution was stirred at room temperature for 3 h (TLC: hexane/ethyl acetate=7:3). The mixture was poured onto ice-water and was extracted with DCM (100 ml). The organic solution was washed twice with sulfuric acid solution (0.05 M), once with water and twice with aq NaHCO$_3$ solution. The organic layer was dried over MgSO$_4$, filtered, and evaporated and the residue was purified by column chromatography using hexane/ethyl acetate=8:2+5% TEA as the eluent. The complete separation of (1′S) (R_f: 0.53) and (1′R) (R_f: 0.44) acetals could not be achieved. The homogeneous fractions were collected and used for spectroscopic characterization, the non-homogeneous fractions weighed 1.060 g.

Yield for the (1′S) acetal: 0.279 g (16%); [α]$_D$ −19.7 (c 0.1, CHCl$_3$); mp: 181–182 °C (EtOH); ^{1}H NMR (200 MHz, CDCl$_3$) δ 8.00–7.80 (4H, m, H-arom.), 7.60–7.44 (3H, m, H-arom.), 7.01 (2H, d, J=9.1 Hz, H-arom.), 6.84 (2H, d, J=9.1 Hz, H-arom.), 6.42 (1H, s, H-acetal), 5.71 (1H, s, H-1), 5.14 (1H, dd, J=7.8 and 10.2 Hz), 4.72 (1H, dd, J=5.1 and 7.8 Hz), 4.44 (1H, d, J=5.1 Hz), 4.09–3.91 (1H, m), 3.78 (3H, s, OMe), 2.18 (3H, s, OAc), 1.21 (d, 3H, J=6.2 Hz, C-5 Me); ^{13}C NMR (200 MHz, CDCl$_3$) δ 170.23 (C acetyl), 155.16, 150.17, 135.50, 133.83, 132.91, 128.49,

128.33, 127.74, 126.55, 126.31, 125.90, 123.52, 117.76, 114.69, 103.39 (C acetal), 96.28 (C-1), 77.27, 75.73, 71.50, 64.54 (C-2 to C-5), 55.65 (OMe), 21.00 (C acetyl), 17.10 (C-6). Calcd for [M+Na]$^+$ 473.157, found mass for C$_{26}$H$_{26}$O$_7$ [M+Na]$^+$ 473.158.

Yield for the (1′R) acetal: 0.226 g (13%); [α]$_D$ −17.2 (c 0.2, CHCl$_3$); mp: 125–128 °C (EtOAc–hexane); ^{1}H NMR (200 MHz, CDCl$_3$) δ 8.07 (1H, s, H-arom.), 7.98–7.82 (3H, m, H-arom.), 7.71 (1H, dd, H-arom.), 7.55–7.45 (2H, m, H-arom.), 7.03 (2H, d, J=9.1 Hz, H-arom.), 6.84 (2H, d, J=9.1 Hz, H-arom.), 6.13 (1H, s, H-acetal), 5.76 (1H, s, H-1), 5.10 (1H, dd, J=6.8, 10.0 Hz), 4.62–4.48 (2H, m), 4.08–3.92 (1H, m), 3.77 (3H, s, OMe), 2.13 (3H, s, OAc), 1.16 (d, 3H, J=6.6 Hz, C-5 Me); ^{13}C NMR (200 MHz CDCl$_3$) δ 169.88 (C acetyl), 155.13, 150.09, 135.50, 134.05, 133.75, 133.00, 128.47, 128.30, 127.71, 126.90, 126.58, 126.20, 125.90, 123.99, 123.53, 117.74, 114.69, 104.96 (C acetal), 96.06 (C-1), 78.10, 75.68, 74.84, 64.92 (C-2 to C-5), 55.62 (OMe), 21.00 (C acetyl), 17.12 (C-6). Calcd for [M+Na]$^+$ 473.157, found mass for C$_{26}$H$_{26}$O$_7$ [M+Na]$^+$ 473.159.

4.2.7. (1′R)-p-Methoxyphenyl 2,3-di-O-acetyl-4,6-O-(2-naphthyl)ethylidene-β-D-glucopyranoside [(1′R)-11]

To a suspension of 10 (175 mg, 0.62 mmol) in DMF (5 ml), 2-(1,1-dimethoxyethyl)naphthalene (6) (710 mg, 3.29 mmol) and a catalytic amount of (+)-10-camphorsulfonic acid (87 mg, 0.348 mmol) were added and the mixture was stirred at room temperature for 3 h. The mixture was neutralized with triethylamine and evaporated in vacuum. Then diethyl ether was added to the mixture and washed with brine (3×). The organic layer was dried (MgSO$_4$), filtered, and concentrated in vacuum. The residue was purified by column chromatography (hexane/ethyl acetate=1:1) to give a foam (93 mg, 35%), which was treated with pyridine (1 ml) and acetic anhydride (1 ml) for 12 h at room temperature. Then the solution was slowly quenched with aqueous 10% HCl and extracted with ethyl acetate (3×10 ml). The organic layer was washed with saturated aqueous solution of NaHCO$_3$ (3×) and brine, dried (MgSO$_4$), filtered, and concentrated in vacuum to give a foam (101 mg, 91%), which was crystallized from cyclohexane (mp: 159–161 °C). [α]$_D$ +7.1 (c 0.4, CHCl$_3$); IR ν_{max} (KBr) 2956, 2898, 1748, 1508, 1372, 1220, 1128, 1074, 1034, 830, 754 cm^{-1}; ^{1}H NMR (500 MHz, CDCl$_3$) δ 7.97–7.47 (m, 7H, H-naphthyl), 6.93 (dd, 2H, J=9.1, <1 Hz, H-arom.), 6.81 (dd, 2H, J=9.1, <1 Hz, H-arom.), 5.38 (t, 1H, J=9.4 Hz, H-3), 5.28 (t, 1H, J=7.9 Hz, H-2), 5.01 (d, 1H, J=7.9 Hz, H-1), 4.12 (m, 2H, H-6), 4.04 (t, 1H, J=9.4 Hz, H-4), 3.76 (s, 3H, OMe), 3.57 (m, 1H, H-5), 2.16 (s, 3H, OAc), 2.09 (s, 3H, OAc), 1.80 (s, 3H, acetal Me); ^{13}C NMR (125 MHz, CDCl$_3$, 25 °C) δ 170.2 (C acetyl), 169.6 (C acetyl), 155.8 (C-q phenyl), 150.9 (C-q phenyl), 140.6 (C-q naphthyl), 133.1 (C-q naphthyl), 132.9 (C-q naphthyl), 128.5–123.1 (7×C-t naphthyl), 118.6 (2×C-t phenyl), 114.6 (2×C-t phenyl), 100.9 (C-1), 100.5 (C acetal), 72.3 (C-2, C-3), 70.9 (C-4), 67.8 (C-5), 62.5 (C-6), 55.6 (OMe), 22.6 (Me), 20.9

(C acetyl), 20.7 (C acetyl). Calcd for $[M+Na]^+$ 545.178, found mass for $C_{29}H_{30}O_9$ $[M+Na]^+$ 545.180.
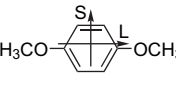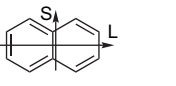
4.2.8. (1'S)-p-Methoxyphenyl 2,3-di-O-acetyl-4,6-O-(1-naphthyl)ethylidene-β-D-glucopyranoside [(1'S)-12a] and (1'R)-p-methoxyphenyl 2,3-di-O-acetyl-4,6-O-(1-naphthyl)ethylidene-β-D-glucopyranoside [(1'R)-12b]

To a suspension of **10** (286 mg, 1 mmol) in DMF (5 ml), 1-(1,1-dimethoxyethyl)naphthalene (**7**) (276 mg, 1.3 mmol) and a catalytic amount of p-toluenesulfonic acid (19 mg, 0.1 mmol) were added and the mixture was stirred at room temperature for 40 h. The mixture was neutralized with TEA and evaporated in vacuum. Then diethyl ether was added to the mixture and washed with water ($3\times$). The organic layer was dried ($MgSO_4$), filtered, and concentrated in vacuum. The residue was purified by column chromatography (hexane/ethyl acetate=1:1) to give a foam (102 mg, 23%), which was treated with pyridine (0.5 ml) and acetic anhydride (0.5 ml) for 12 h at room temperature. Then the solution was slowly quenched with aqueous 10% HCl and extracted with ethyl acetate (3×10 ml). The organic layer was washed with saturated aqueous solution of $NaHCO_3$ ($3\times$) and brine, dried ($MgSO_4$), filtered, and concentrated in vacuum to give a foam (94.5 mg, 84%), which was crystallized from hexane/ethyl acetate=10:1 to give (1'S)-**12a** (mp: 154–156 °C). $[\alpha]_D$ −78.3 (c 0.1, $CHCl_3$); IR ν_{max} (KBr) 3048, 2954, 1750, 1508, 1374, 1246, 1222, 1176, 1106, 1084, 1036, 760 cm^{-1}; ^1H NMR (500 MHz, $CDCl_3$) δ 7.90–7.44 (m, 7H, H-naphthyl), 6.85 (dd, 2H, J=8.8, <1 Hz, H-arom.), 6.68 (dd, 2H, J=8.8, <1 Hz, H-arom.), 5.37 (t, 1H, J=8.1 Hz, H-3), 5.01–4.96 (m, 2H, H-1+H-2), 4.12 (m, 1H, H-6a), 3.79 (m, 1H, H-6b), 3.76 (s, 3H, OMe), 3.68 (m, 1H, H-5), 3.67 (m, 1H, H-4), 2.18 (s, 3H, OAc), 2.04 (s, 3H, OAc), 1.78 (s, 3H, acetal Me); ^{13}C NMR (125 MHz, $CDCl_3$, 25 °C) δ 170.3 (C acetyl), 169.4 (C acetyl), 155.8 (C-q phenyl), 150.9 (C-q phenyl), 134.9 (C-q naphthyl), 134.3 (C-q naphthyl), 130.7 (C-q naphthyl), 129.8–125.1 ($7\times$C-t naphthyl), 118.8 ($2\times$C-t phenyl), 114.5 ($2\times$C-t phenyl), 103.4 (acetal), 100.7 (C-1), 72.4–72.0 (C-2 to C-4), 67.0 (C-5), 63.1 (C-6), 55.6 (OMe), 30.2 (Me), 21.0 (C acetyl), 20.6 (C acetyl). Calcd for $[M+Na]^+$ 545.178, found mass for $C_{29}H_{30}O_9$ $[M+Na]^+$ 545.180.

For the spectroscopic identification of (1'R)-**12b**, 50 mg of the foam were purified by preparative TLC (hexane/ethyl acetate=2:1). ^1H NMR (200 MHz, $CDCl_3$) δ 8.44–8.39 (m, 1H, H-naphthyl), 7.87–7.79 (m, 3H, H-naphthyl), 7.48–7.41 (m, 3H, H-naphthyl), 6.93–6.77 (m, 4H, H-phenyl), 5.39 (t, 1H, J=9.2 Hz), 5.29 (t, 1H, J=9.2 Hz), 4.20 (t, 1H, J=9.2 Hz), 4.10–4.03 (m, 2H), 3.76 (s, 3H, OMe), 3.64–3.55 (m, 1H), 2.19 (s, 3H, OAc), 2.09 (s, 3H, OAc), 1.93 (s, 3H, acetal Me); ^{13}C NMR (50 MHz, $CDCl_3$, 25 °C) δ 170.1 (C acetyl), 169.6 (C acetyl), 155.8 (C-q phenyl), 150.9 (C-q phenyl), 138.4 (C-q naphthyl), 134.4 (C-q naphthyl), 129.9 (C-q naphthyl), 129.4–124.1 ($7\times$C-t naphthyl), 118.6 ($2\times$C-t phenyl), 114.6 ($2\times$C-t phenyl), 101.3 (acetal), 100.9 (C-1), 72.3–67.8 (C-2 to C-5), 62.5 (C-6), 55.6 (OMe), 23.4 (Me), 20.8 (C acetyl), 20.7 (C acetyl). Calcd for $[M+Na]^+$ 545.178, found mass for $C_{29}H_{30}O_9$ $[M+Na]^+$ 545.179.

Table 3
Spectral parameters for 1,4-dimethoxybenzene (DMB) and naphthalene used in DeVoe calculations

	Band	Calculated[a]			Experimental[b]			
		λ_{max} (nm)	f	Pol.	λ_{max} (nm)	ν (kK)	$\Delta\nu$ (kK)	D (D^2)
(DMB structure)	^1L_b	289.0	0.06	L	288	34.7	2.6	2.3
	^1L_a	256.2	0.19	S	224	44.7	3.6	7.0
	^1B_b	208.4	0.67	L	193	51.5[c]	2.5[c]	10.0[c]
	^1B_a	207.2	0.83	S		51.8[c]	2.5[c]	12.0[c]
(naphthalene structure)	^1L_b	315.3	0.004	L	312	32.0	nc	nc[d]
	^1L_a	296.5	0.15	S	276	36.2	4.0	5.4
	^1B_b	235.3	1.65	L	220	45.4	2.0[e]	45.0[e]
	^1B_a	225.9	0.57	S		47.6[e]	2.0[e]	12.0[e]

[a] ZINDO/S calculations on B3LYP/6–31G(d) optimized structures (DMB in C_{2h} symmetry); f, oscillator strength; Pol.: polarization direction as indicated in the diagrams (L, long axis; S, short axis).
[b] From UV spectra in acetonitrile, concentrations 1.16 mM (DMB) and 1.39 mM (naphthalene), 0.01 cm cell. Legend: ν, transition frequency in kK (10^3 cm^{-1}); $\Delta\nu$, half-height bandwidth in kK; D, dipole strength in square Debye (1 $D^2=10^{-36}$ cgs). These values were used in DeVoe calculations.
[c] Values calculated with two-Gaussians fit of the absorption band, assuming a frequency separation of 0.3 kK as found by ZINDO.
[d] Not considered in the calculations.
[e] Band ^1B_a appearing as a short-wavelength shoulder on the most intense one.[32] Parameters calculated assuming a frequency separation of 1.7 kK as found by ZINDO.

4.3. Computational section

DeVoe calculations were run with a Fortran program written by Hug,[31] using MMFF-optimized geometries or solid-state structures as input. Spectral parameters for transition dipoles (reported in Table 3) were extracted from UV spectra of 1,4-dimethoxybenzene (DMB) and naphthalene in acetonitrile, supported by ZINDO calculations on DFT-optimized structures. Dipoles were placed in the center or respective chromophores. For DeVoe calculations of cell clusters, the DMB or naphthalene chromophore in a central molecule was allowed to couple with all chromophores belonging to distinct molecules at distances <10 Å (center-to-center).

MMFF conformational searches and AM1 calculations were run using Spartan'06, Wavefunction, Inc, Irvine CA, with default parameters and convergence criteria. ZINDO and DFT calculations were run using Gaussian'03 W, Revision D.01, Gaussian, Inc., Pittsburgh PA. DFT geometry optimizations were executed with B3LYP/6-31G(d) method, using an input C_{2h}-symmetric structure for DMB and D_{2h}-symmetric structure for naphthalene.

References and notes

1. Paulsen, H. Angew. Chem., Int. Ed. Engl. **1990**, 29, 823–839.
2. Schmidt, R. R.; Kinzy, W. Adv. Carbohydr. Chem. Biochem. **1994**, 50, 21–123.

3. Lipták, A.; Szurmai, Z.; Oláh, V. A.; Harangi, J.; Szabó, L.; Nánási, P. *Carbohydr. Res.* **1985**, *138*, 1–15.

4. Lipták, A.; Borbás, A.; Jánossy, L.; Szilágyi, L. *Tetrahedron Lett.* **2000**, *41*, 4949–4953.

5. Borbás, A.; Szabó, Z. B.; Szilágyi, L.; Bényei, A.; Lipták, A. *Tetrahedron* **2002**, *58*, 5723–5732.

6. Kurtán, T.; Borbás, A.; Szabó, B. Z.; Lipták, A.; Bényei, A.; Antus, S. *Chirality* **2004**, *16*, 244–250.

7. Kónya, K.; Kurtán, T.; Kiss-Szikszai, A.; Juhász, L.; Antus, S. *Arkivoc* **2004**, *XIII*, 72–78.

8. Kiss, L.; Kurtán, T.; Antus, S.; Bényei, A. *Chirality* **2003**, *6*, 558–563.

9. Antus, S.; Kurtán, T.; Juhász, L.; Kiss, L.; Hollósi, M.; Májer, Zs. *Chirality* **2001**, *13*, 493–506.

10. Borbás, A.; Szabó, B. Z.; Szilágyi, L.; Bényei, A.; Lipták, A. *Cabohydr. Res.* **2002**, *337*, 1941–1951.

11. Harada, N.; Nakanishi, K. *Circular Dichroic Spectroscopy, Exciton Coupling in Organic Stereochemistry*; Oxford University Press: Oxford, 1983.

12. (a) Berova, N.; Nakanishi, K. Exciton Chirality Method: Principles and Application. In *Circular Dichroism: Principles and Applications*, 2nd ed.; Nakanishi, K., Berova, N., Woody, R. W., Eds.; Wiley-VCH: New York, NY, 2000; Chapter 12, pp 337–382; (b) Berova, N.; Di Bari, L.; Pescitelli, G. *Chem. Soc. Rev.* **2007**, *36*, 914–931.

13. Schreder, B.; Lukacs, Z.; Schmitt, M.; Schreier, P.; Humpf, H.-U. *Tetrahedron: Asymmetry* **1996**, *7*, 1543–1546.

14. (a) DeVoe, H. *J. Chem. Phys.* **1964**, *41*, 393–400; (b) DeVoe, H. *J. Chem. Phys.* **1965**, *43*, 3199–3208.

15. (a) Di Bari, L.; Pescitelli, G.; Reginato, G.; Salvadori, P. *Chirality* **2001**, *13*, 548–555; (b) Pescitelli, G.; Gabriel, S.; Wang, Y.; Fleischhauer, J.; Woody, R. W.; Berova, N. *J. Am. Chem. Soc.* **2003**, *125*, 7613–7628; (c) Superchi, S.; Giorgio, E.; Rosini, C. *Chirality* **2005**, *16*, 422–451.

16. Hussain, H.; Krohn, K.; Flörke, U.; Schulz, B.; Draeger, S.; Pescitelli, G.; Antus, S.; Kurtán, T. *Eur. J. Org. Chem.* **2007**, 292–295.

17. Krohn, K.; Kock, I.; Elsässer, B.; Flörke, U.; Schulz, B.; Draeger, S.; Pescitelli, G.; Antus, S.; Kurtán, T. *Eur. J. Org. Chem.* **2007**, 1123–1129.

18. Krohn, K.; Zia-Ullah; Hussain, H.; Flörke, U.; Schulz, B.; Draeger, S.; Pescitelli, G.; Salvadori, P.; Antus, S.; Kurtán, T. *Chirality* **2007**, *19*, 464–470.

19. Krohn, K.; Farooq, U.; Flörke, U.; Schulz, B.; Draeger, S.; Pescitelli, G.; Salvadori, P.; Antus, S.; Kurtán, T. *Eur. J. Org. Chem.* **2007**, *19*, 3206–3211.

20. Hussain, H.; Krohn, K.; Flörke, U.; Schulz, B.; Draeger, S.; Pescitelli, G.; Salvadori, P.; Antus, S.; Kurtán, T. *Tetrahedron: Asymmetry* **2007**, *18*, 925–930.

21. Dai, J.; Krohn, K.; Elsässer, B.; Flörke, U.; Draeger, S.; Schulz, B.; Pescitelli, G.; Salvadori, P.; Antus, S.; Kurtán, T. *Eur. J. Org. Chem.* **2007**, *29*, 4845–4854.

22. Kurtán, T.; Pescitelli, G.; Salvadori, P.; Kenéz, Á.; Antus, S.; Illyés, T.-Z.; Szilágyi, L.; Szabó, I. *Chirality* **2008**, doi:10.1002/chir.20458 published online.

23. (a) Kuroda, R.; Honma, T. *Chirality* **2000**, *12*, 269–277; (b) Kuroda, R. Solid-State CD: Application to Inorganic and Organic Chemistry. In *Circular Dichroism*; Berova, N., Nakanishi, K., Woody, R. W., Eds.; Wiley-VCH: New York, NY, 2000; pp 159–184.

24. Harms, K.; Wocadlo, S. *XCAD4-CAD4 Data Reduction*; University of Marburg: Marburg, Germany, 1995.

25. Lehman, M. S.; Larsen, F. K. *Acta Crystallogr., Sect. A* **1974**, *30*, 580–584.

26. Altomare, A.; Cascarano, G.; Giacovazzo, C.; Guagliardi, A. *J. Appl. Crystallogr.* **1993**, *26*, 343–350.

27. Sheldrick, G. M. *SHELX-97. Programs for Crystal Structure Analysis (Release 97-2)*; Institüt für Anorganische Chemie der Universität: Göttingen, Germany, 1998.

28. Farrugia, L. J. *WINGX-97 System*; University of Glasgow: UK, 1996.

29. ORTEP3 for Windows: Farrugia, L. J. *J. Appl. Crystallogr.* **1997**, *30*, 565.

30. PLATON/PLUTON: (a) Spek, A. L. *Acta Crystallogr.* **1990**, *A46*, C34; (b) Spek, A. L. *PLATON, A Multipurpose Crystallographic Tool*; Utrecht University: Utrecht, The Netherlands, 1998.

31. Cech, C. L.; Hug, W.; Tinoco, I., Jr. *Biopolymers* **1976**, *15*, 131–152.

32. Rubio, M.; Merchán, M.; Ortí, E.; Roos, B. O. *Chem. Phys.* **1994**, *179*, 395–409.